



Published in final edited form as:

J Biomed Mater Res A. 2014 September ; 102(9): 3102–3111. doi:10.1002/jbm.a.34983.

Undifferentiated Human Adipose-derived Stromal/Stem Cells loaded onto Wet-Spun Starch-polycaprolactone Scaffolds Enhance Bone Regeneration: Nude Mice Calvarial Defect *in vivo* Study

Pedro P. Carvalho^{1,2,3}, Isabel B. Leonor^{2,3}, Brenda J. Smith⁵, Isabel R. Dias^{2,3,4}, Rui L. Reis^{2,3}, Jeffrey M. Gimble¹, and Manuela E. Gomes^{2,3}

¹Stem Cell Biology Laboratory, Pennington Biomedical Research Center, Louisiana State University System, Baton Rouge, LA, USA

²3B's Research Group – Biomaterials, Biodegradables and Biomimetics, University of Minho, Headquarters of the European Institute of Excellence on Tissue Engineering and Regenerative Medicine, Avepark, Guimarães, Portugal

³ICVS/3B's PT Government Associated Lab, Braga/Guimarães, Portugal

⁴Department of Veterinary Sciences, School of Agrarian and Veterinary Sciences, University of Trás-os-Montes e Alto Douro, Vila Real, Portugal

⁵Department of Nutritional Science, Oklahoma State University, Stillwater, OK, USA

Abstract

The repair of large bony defects remains challenging in the clinical setting. Human adipose-derived stromal/stem cells (hASCs) have been reported to differentiate along different cell lineages, including the osteogenic. The objective of the present study was to assess the bone regeneration potential of undifferentiated hASCs loaded in starch-polycaprolactone (SPCL) scaffolds, in a critical-sized nude mice calvarial defect.

Human ASCs were isolated from lipoaspirate of five female donors, cryopreserved and pooled together. Critical-sized (4 mm) calvarial defects were created in the parietal bone of adult male nude mice. Defects were either left empty, treated with an SPCL scaffold alone, or SPCL scaffold with human ASCs. Histological analysis and Micro-CT imaging of the retrieved implants were performed. Improved new bone deposition and osseointegration was observed in SPCL loaded with hASC engrafted calvarial defects as compared to control groups that showed little healing.

Non differentiated human ASCs enhance ossification of non-healing nude mice calvarial defects, and wet-spun SPCL confirmed its suitability for bone tissue engineering. This study supports the potential translation for ASC use in the treatment of human skeletal defects.

Corresponding author: Pedro P. Carvalho, DVM, PhD, pedro.carvalho@dep.uminho.pt, Address: 3B's Research Group, Avepark, Zona Industrial da Gandra, S.Cláudio do Barco, 4806-909 Caldas das Taipas - Guimarães, Portugal, Phone: +351 (253) 510 913, Fax: +351 (253) 510909.

Disclosure of Interest

The authors declare that they have no competing interest.

Keywords

Adipose-derived Stem Cells; SPCL; Calvarial defect; Critical size defect; Bone regeneration

1. Introduction

The currently available options for skeletal tissue regeneration fall short of the ideal reconstructive methods. Autogenous grafts or alloplastic materials that are applied surgically have inherent disadvantages such as unnatural texturing, inflammation, extrusion, resorption, and even rejection. They have limited availability, substantive morbidity, and may demonstrate poor viability^{1,2}. Thus, it remains a pressing need for a suitable alternative therapy for bone tissue repair. Our laboratory and others have focused on harnessing the osteogenic capability of adipose-derived stromal cells (ASCs) seeded/cultured onto adequate scaffolds, for the eventual repair of non-healing skeletal defects^{3,4}.

ASCs offer several advantages over other multipotent cells (such as bone marrow mesenchymal cells - BMSCs) for tissue engineering purposes⁵⁻⁷. They are available in large numbers, are easily accessible, and attach and proliferate rapidly in culture. They have been described as mesenchymal stromal cells, with a proven ability to differentiate along osteogenic, adipogenic, chondrogenic and myogenic cell types, among others⁸⁻¹³. Moreover, hASCs show robust mineralization within 9 to 12 days of *in vitro* differentiation^{10,14}. Previous studies have attempted to utilize hASCs for the regeneration of skeletal defects¹⁵⁻¹⁷. Previous studies have reported that allogenic mesenchymal stromal/stem cells (MSCs) either derived from bone marrow or from circulative MSCs could be isolated and cultured in advance to achieve suitable implantation in clinical applications¹⁸⁻²⁰. However, the higher number of ASCs that can be isolated in one single step allows a more straightforward application of these cells particularly when time is of critical importance. Our study sought to assess the capacity of undifferentiated human ASCs loaded onto wet-spun SPCL scaffolds to regenerate a non-healing mouse calvarial defect.

A number of studies have used a calvarial model to assess bone tissue engineered constructs comprised of stem cells in combination with natural and synthetic scaffolds²¹⁻²⁹. Most of the studies reported in literature use ASCs pre-differentiated onto the osteogenic lineage prior to implantation, or a combination of ASCs and growth factors such as bone morphogenetic protein - 2 (BMP-2) to enhance bone healing³⁰. Few studies report the use of non-differentiated ASCs but combined with ceramic osteoinductive materials or bone grafts³¹. In this study we have used for the first time wet-spun SPCL scaffolds loaded with undifferentiated ASCs to assess bone regeneration. Scaffolds used for bone tissue engineering are expected to provide mechanical support and to serve as a substrate where cells can attach, and subsequently proliferate and undergo differentiation³². In the present study a scaffold based on a polymeric blend of starch poly(ϵ -caprolactone) (SPCL) was selected, processed by wet-spinning, which proved to be biocompatible and biodegradable³³ and also able to support adhesion, proliferation and osteogenic differentiation of seeded hASCs^{33,34}. The addition of starch to the poly-caprolactone (PCL) improves the mechanical properties, providing higher resistance of the blend to tensile forces, and therefore closer similarity to those found in native bone. PCL degradation rates

also benefit with the inclusion of starch, being easily degraded over a shorter period of time although still remaining for up to three months after implantation, and therefore the entire new bone formation process. In an effort to address the bench to bedside application of ASCs in regenerative medicine, the use of non-differentiated ASCs of human origin combined with wet-spun SPCL scaffolds was assessed in a murine calvarial defects model. To avoid incompatibility of xenografted tissue, an athymic mouse model was utilized (Charles Rivers)³⁵.

2. Material and Methods

2.1. Patient Enrollment

All studies were performed with informed consent of patients under a protocol reviewed and approved by the Pennington Biomedical Research Center Institutional Review Board (PBRC #23040). Five female donors of Western European descent with a mean (\pm SD) age and BMI of 30.0 ± 7.9 years and 25.1 ± 3.9 , respectively, were enrolled in the study.

2.2. ASCs isolation and seeding

Cells were isolated from human lipoaspirates and expanded as previously described³⁶. Cryopreserved vials with 1×10^6 ASCs (P0) isolated from 5 donors were thawed, pooled together and seeded in five 175cm² culture flasks. Adherent cells were maintained in stromal medium [DMEM/Hams F-12 medium supplemented with 10% FBS (Hyclone, Logan, Utah, USA) and 1% antibiotic/antimycotic] until 80–90% confluence. At this point cells were harvested using TrypLE Express (Invitrogen, Carlsbad, CA, USA)³⁷ and resuspended in stromal medium to neutralize the enzymatic digestion. Next, 10 μ L aliquots were diluted with 10 μ L of trypan blue and cells were assessed for viability and counted using a hemocytometer, and used for scaffold loading and characterization assays.

2.3. Flow Cytometry

After culturing the pool of ASCs until confluence (80–90%), cells were harvested using TrypLE Express (Invitrogen, Carlsbad, CA, USA)³⁷, washed three times with PBS and aliquots of 10^5 cells were incubated with phycoerythrin-conjugated monoclonal antibodies directed against: CD29 (eBioscience Cat. No. 12-0297), CD34 (Becton Dickinson Cat. No. 348057), CD44 (BD Cat. No. 348057), CD45 (eBioscience Cat. No. 12-0459), CD73 (BD Pharmingen Cat. No. 550257), CD90 (BD Pharmingen Cat. No. 55596), CD105 (eBioscience Cat. No. 12-1057) and IgG1 κ control (BD Pharmingen Cat. No. 554679) for 20 min on ice before being washed three times with PBS supplemented with 1% bovine serum albumin and fixed in 1% formaldehyde overnight at 4°C^{14,38,39}. For each sample, 10^5 events were collected in triplicates on a Becton Dickinson FACScalibur flow cytometer using CELLQuest acquisition software (Becton Dickinson) and analyzed using Flow Jo software (Tree Star). This antibody panel was selected, in part, based on the International Society for Cell Therapy position paper on the criteria for defining mesenchymal stromal cells⁴⁰.

2.4. ASCs differentiation assay

2.4.1. Adipogenic differentiation—A twelve well plate was seeded at approximately 3.3×10^4 cells per square centimeter of the pool of ASCs (P1) and allowed to reach confluence (80–90%). At this point, confluent cultures were induced with adipogenic differentiation medium [DMEM/Hams F-12, 3% FBS, 1% antibiotic/antimycotic, 0.5mM isobutylmethylxanthine, 33mM biotin, 17mM pantothenate, 5 μ M troglitazone (Sigma), 1mM dexamethasone, 10mM insulin] for 3 days before being converted to adipocyte maintenance medium (identical to adipogenic differentiation medium without isobutylmethylxanthine and troglitazone) ^{36,41}. Cells were maintained for 9 days, with medium changes every third day, before fixation and Oil Red O staining.

2.4.2. Osteogenic differentiation—Confluent cultures of the pool of ASCs (P1) seeded in twelve-well plates at approximately 3.3×10^4 cells per square centimeter, were converted to osteogenic medium (DMEM/Hams F-12 or DMEM, 10% FBS, 1% antibiotic/antimycotic, 10mM β -glycerophosphate, 50 μ g/ml sodium 2-phosphate ascorbate, 10^{-8} M dexamethasone) and maintained in culture for 12 days with medium changes every third day. These cultures were rinsed three times with 150mM NaCl, fixed in 70% ethanol, and stained with Alizarin Red ⁴².

2.5. Scaffold preparation

The scaffolds were prepared using a processing methodology that has been previously described in detail ^{43,44}. Briefly, a biodegradable thermoplastic blend of corn starch with polycaprolactone (30:70 wt%), designated as SPCL (Novamont, Italy), was dissolved in chloroform at a concentration of 30% w/v. The obtained polymer solution was loaded into a plastic syringe (5ml), with a metallic needle (internal diameter 0.8mm) attached to it. The syringe was connected to a programmable syringe pump (KD Scientific, World Precision Instruments, UK) to inject the polymer solution at a controlled pumping rate, thus allowing the formation of the fiber mesh directly into the coagulation bath consisting of methanol. The fiber mesh structure was formed during the processing by the random movement of the coagulation bath ^{33,43}. These fibers have approximately $195 \pm 24.6\mu$ m of thickness. The formed scaffolds were then air dried at room temperature overnight in order to remove any remaining solvents. The scaffolds were cut into 4mm diameter discs using a metallic punch, followed by ethylene oxide sterilization before *in vitro* seeding/*in vivo* implantation.

2.6. Scaffold loading

Scaffold samples with 4mm diameter and 1mm thickness were placed in a 48 well plate, and each one loaded with 50 μ l of a cell suspension containing 0.5×10^6 cells. The plate with the scaffolds was placed inside an incubator (37°C and 5% CO₂) overnight to allow cell attachment. An equal number of scaffolds was left without cells but immerse in the same volume of culture medium over the same period of time (overnight).

2.7. Calvarial defect – surgical procedure

The experimental protocol was performed in accordance with Pennington Biomedical Research Center Animal Care and Use Committee approved protocols. For the cranial defect

model, a total of 18 mice (nine for each time point) were anesthetized with inhalant isoflurane. The skin over the skull was cleaned with Nolvasam and 70% ethanol. Bupivacaine/lidocaine was injected at the surgical site. Incisions of 20mm length were made over the sagittal suture and the skin, musculature, and periosteum was reflected. Two full thickness bone defects (one on each side of the sagittal suture) of 4mm diameter (each) were trephined in the center of the parietal bone using a hand held Dremel drill equipped with a sterile drill bit, very carefully to insure that the dura mater was not damaged. The surgical area was irrigated with 0.9% NaCl solution throughout the procedure. Defects were assigned to the following groups (n=6 defects for each group in each time point): Empty defect; SPCL scaffold alone; SPCL scaffold plus human ASCs. Following implantation of the scaffolds, the skin was closed with metal clips. Animals were placed on a heating pad under a warming light and observed until they recovered consciousness. After recovering consciousness animals were monitored for 30 minutes to assess evidence of distress. Animals received analgesia preoperatively (Bupivacaine/Lidocaine) and during the postoperative period (Carprofen) as needed based on evidence of discomfort, evaluated by animal behavior, feeding, and vocalization. Wound clips were removed 7–10 days post-operatively, after evaluation for adequate wound healing.

After 4 and 8 weeks of implantation, the animals were euthanized by carbon dioxide asphyxiation²⁹, and the heads dissected and kept in a solution of 10% formalin at 4°C for 48h followed by histological analysis and micro-CT scanning.

Experimental groups:

Number of animals (N)	Left defect	Right defect
2	Empty	Empty
4	Empty	SPCL
4	Empty	SPCL+ASCs
2	SPCL	SPCL
4	SPCL	SPCL+ASCs
2	SPCL+ASCs	SPCL+ASCs

2.8. S.E.M. analysis

Cell–scaffold constructs were washed in PBS, fixed in a 2.5% solution of glutaraldehyde (Sigma) overnight, dehydrated in a series of ethanol concentrations (50%, 70%, 90% and 100%) and air-dried before being sputter-coated with gold by ion sputtering. SEM observation was performed to assess the adhesion of ASCs onto the SPCL fiber meshes using a Hitachi SU-70 UHR Schottky (Hitachi, Japan) equipment attached with energy dispersive electron X-ray spectroscopy (Bruker Quantax Esprit 1.8 EDS system, X-flash detector).

2.9. Histological analysis

After fixation with formalin, explants were rinsed with PBS, decalcified using an acidic solution of Immunocal[®] (Decal Chemical Corp, USA). Samples were included in histological cassettes and put in a tissue processor equipment (Microm STP120, MICROM International GmbH, Germany) for dehydration in a series of ethanol concentrations (70%, 80%, 95% and 100%) followed by xylene solution to remove water from tissues. Samples were then embedded in paraffin wax (Microm EC 350-2, ThermoScientific, USA), included in blocks, and stored at room temperature. Blocks were cut into 10 μ m sections using a microtome, and then deparaffinized and stained with Hematoxylin/Eosin and Masson's Trichrome before being mounted for microscopic observation.

2.10. Histomorphometric analysis

Histological sections (n=4 different samples of each experimental group defect) were assessed. Low magnification images (2.5 fold) were used to allow visualizing the entire defect site. Histological slides passing through the center of the defect with a total length of 4mm were chosen and AdobePhotoshop and ImageJ software were used to outline the implant area, designated as region of interest (ROI), and the average percentage of filled area in the defect (newly formed tissue) was calculated. The same procedure was performed for micro-CT images (n=3 scan images of each group).

2.11. Micro-CT scanning

Images of the mice skulls were collected with a μ -CT equipment Scanco *VivaCT* 40 (Scanco Medical), to acquire raw data. Skulls were irradiated using an x-ray voltage of 70kVp/500 μ A, and an exposure time of 1600ms. Raw data was reconstructed into greyscale slice images, and then Amira version 3.1 was used for 3D imaging conversion.

2.12. Statistical analysis

All results are provided as mean \pm standard deviation (SD). One-way ANOVA with Tukey multiple comparison post test assessed statistical significance for histomorphometric analysis on Figures 5 and 6 (** represents $p < 0.01$ and *** represents $p < 0.001$).

3. Results

Flow cytometric analysis with a standard panel of cell surface markers, based on the International Society for Cell Therapy (ISCT) position paper on the criteria for defining mesenchymal stem cells/multipotent stromal cells (MSCs)⁴⁰, evaluated the immunophenotype of ASCs before implantation. Consistently with published reports⁴⁵, the human ASC displayed strong positivity for the stromal markers CD29 (β_1 integrin), CD44, CD73 (5' ecto-nucleotidase), CD90 (Thy-1) and CD105 (endoglin) and low expression of CD34, and CD45 (Fig 1). Differentiation assays with ASCs pooled together, assessed the potential of these cells to differentiate into both adipogenic and osteogenic lineages through staining with Oil Red O and Alizarin Red respectively (Fig 2).

SEM examination showed that ASCs adhered and were well spread on the surface of the SPCL fibers, one day after seeding (Fig 3). ASCs present a characteristic stretched shape,

attaching to the fibers, as oppose to the round shape observed immediately after being harvested, attesting their viability at the time of fixation for imaging. Images also confirmed prior results that assessed the high porosity and interconnectivity of these scaffolds.

Light microscopy analysis of histological samples of the explants 8 weeks post-surgery (Fig 4) revealed that empty defects completely lack new bone formation. A thin membrane of dense connective tissue was visible covering the defect site and there was little or no sign of bone remodeling at the edges of the defect. On defects where SPCL scaffolds were implanted, a thin layer of connective tissue, with minimal inflammatory cells and some surrounding granulation tissue, surrounded the fiber meshes. At the interface of native bone with the defect filled with SPCL fibers, areas of bone reorganization were visible. These areas show disorganized layers of matrix with cells as oppose to those of native bone that are parallel and within concentric organization. Defect sites implanted with SPCL scaffolds loaded with ASCs showed higher staining intensity, demonstrating that new bone deposition in the area was more intense. These results were also observed on the explants after 4 weeks of implantation (see Figure 4), although the stainings were less intense, suggesting lower bone deposition. We also observed that the scaffold loaded with ASCs was thinner after 8 weeks of implantation when compared to scaffold without cells. The presence of inflammatory exudates was not detected, and only few giant cells of foreign body and other inflammatory cells surrounding the fibers were observed (evidenced by dark pink color surrounding the fibers). It was possible to see extensive areas of new tissue deposition as well as osseointegration of the fibers that were surrounded by immature trabecular bone, particularly on the edges of the defect (black arrows on Fig 5).

Histomorphometric measurements (Fig 5) confirmed that groups implanted with SPCL loaded with ASCs displayed significantly increased new tissue formation. The Region of Interest (ROI) was determined within slide images passing through the center of the defect area. New tissue formation over the total area of the defect at 4 and 8 weeks respectively, was of 20.84 ± 1.32 and $42.94\% \pm 2.49$ (SPCL + ASCs); $15.25\% \pm 1.29$ and $25.81\% \pm 1.65$ (SPCL); and $8.14\% \pm 1.01$ and $12.95\% \pm 3.16$ (empty).

It is visible in the 3D reconstructed micro-CT images, 8 weeks after implantation, that SPCL scaffolds loaded with ASCs promoted enhanced deposition of mineralized matrix on the defect sites as compared to SPCL scaffold alone. Defects that were left empty showed no signs of mineralization (Fig 6, A–C). Morphometric analysis of the images revealed significant differences ($p < 0.01$) between SPCL + ASCs and the other 2 groups, as well as between SPCL alone and the empty group, assessing the percentage of dense tissue inside the defect area. SPCL + ASCs showed around 70% of new bone formation against, 40% of SPCL alone, and only 5% on empty defects (Fig 6, D).

4. Discussion

Bone tissue engineering strategies using stem cell-based approaches still need to address some challenges before they can be successfully translated to the clinic. One of these is the low yield of autologous cells and the lack of standardized methods for isolation and

expansion of bone progenitor cells. This study extends previous reports on the potential use of human ASCs for bone tissue repair and regeneration.

ASCs can be isolated in high numbers since there is great availability of adipose tissue samples, and are easily expanded *in vitro*¹⁴. Previous studies have demonstrated ASCs ability to differentiate into different cell lineages^{10,46}, including the osteogenic, which supports their potential as an alternative stem cell for bone tissue engineering therapies. The differentiation potential of these cells was assessed for both adipogenic and osteogenic lineages (Figure 2). The induction to chondrogenic lineage was not performed since high numbers of cells are needed to achieve each pellet, and that would imply expanding ASCs for a longer period, and use them in later passages. Previous work in our group assessed the ability of stem cells to differentiate towards the osteogenic lineage *in situ* when loaded onto wet-spun SPCL scaffolds⁴³. The present study focused on the use of undifferentiated ASCs in order to have less manipulation and provide a time saving approach to the clinical application of these cells.

The ease of harness as well as the high number of cells that can be isolated from each liposuction procedure established ASCs as an optimal strategy for autologous applications. An autologous approach avoids immune responses that might jeopardize the recipient and also avoids adverse effects in the bone regeneration process. Still, it is necessary to incorporate these cells in a material with suitable biomechanical properties as well as osteoconductivity. For bone regeneration purposes, the ideal scaffold material is considered to be bioactive, slowly biodegradable, moldable and easy to apply^{47,48}. Other characteristics of the scaffold material to take into consideration are an adequate porosity, and interconnectivity between pores to sustain bone and vascular ingrowth⁴⁸.

In this study, a blend of starch with polycaprolactone (SPCL) obtained by wet-spinning technique was used. Previous *in vitro* characterization studies suggest that SPCL fiber meshes exhibit suitable mechanical properties for bone repair^{33,43}, high interconnectivity within the porous network (porosity around 85%) that seems to benefit cell ingrowth enabling access to nutrients, as well as the removal of metabolic wastes. Other studies support the potential suitability of SPCL scaffolds (obtained by a different method) for the vascularization process in bone tissue engineering⁴⁹. An *in vivo* study from our group has determined that SPCL produced by wet-spinning technique induces little inflammatory response after subcutaneous and intramuscular implantation³⁴. These outcomes coupled with the results from recent studies^{33,43} using SPCL scaffolds produced by wet-spinning and other techniques, reveal promising potential of these fiber meshes for bone tissue engineering. The functionalization of SPCL with the incorporation of calcium and/or silica groups may help to improve its properties and further enhance the potential of this biomaterial for bone regeneration approaches.

The data indicates that the presence of ASC improved the osteogenic function of SPCL implants. Histological staining of the retrieved explants after 8 weeks of implantation revealed that ASCs loading promoted significantly better bone deposition and that the SPCL fibers were better integrated and surrounded by new tissue particularly at native bone/defect interface. Although the defects were not completely bridged, new bone was present in the

center of the defect, with large areas of matrix and connective tissue formation, confirmed by Masson's Trichrome staining and representative micro-CT scanning, particularly in SPCL + ASCs explants. Most of the similar studies reported in literature, use stem cells that are pre-differentiated into the osteogenic lineage prior to implantation^{22,50–53}. This study demonstrates that non-differentiated ASCs enhance the process of bone regeneration when used in tissue engineering strategies. It is debatable if the implanted cells directly achieve these outcomes, or if they recruit surrounding cells (through secreted metabolites) that enhance the regeneration process; it is however clear that the presence of these cells significantly improves the entire process. Bone regeneration is enhanced, therefore saving time and resources, allowing a more straightforward translation to clinical applications. When comparing the effect that scaffolds alone and ASCs loaded onto scaffolds have on bone regeneration, most studies report the same range of improvement, from approximately 20 % to 75–80 % when cells are combined with suitable biomaterials^{22,50,51,53}. Studies using ASCs pre-differentiated onto osteogenic⁵⁴ and endothelial cell lines in combination with bone allografts⁵⁵, report better vascularization when endothelial cell are used but no significant difference in bone regeneration when comparing implants with these last ones and osteogenic or undifferentiated cells. Different studies concluded that pre-differentiation of ASCs in osteogenic lineages will enhance bone regeneration in critical size defects when compared to undifferentiated ASCs, and although using growth factors (BMP-2)^{22,56}, demineralized bone matrix³⁰ or cadaveric processed bone⁵⁷, the percentage of new bone formation does not differ significantly from the one achieved by undifferentiated ASCs combined with suitable scaffolding³¹. Furthermore, the time and resources that prior processing of the cells entails or the clinical implications in situations where time is a critical factor, are not overcome with these type of approaches. Despite the differences in the treatment of the cells or the biomaterials that are applied, one common feature reported by these different studies is that overall the usage of cells overcomes the results that material alone may provide. This study extends and confirms this idea.

5. Conclusion

In summary, histological analysis showed that the bone regeneration process starts from the edges of the defect, and that when ASCs are loaded onto the SPCL scaffolds, this regeneration is enhanced. SPCL wet-spun fibers confirmed to be a suitable and biocompatible material for adipose-derived stem cell loading and implantation in bone regeneration strategies. These findings support the potential use of undifferentiated ASCs in combination with biomaterial scaffolds as an alternative for the repair of large bone defects and as a promising alternative for bone regenerative approaches.

Acknowledgments

P.P.C. acknowledges the Portuguese Foundation for Science and Technology (FCT) for a PhD scholarship (SFRH/BD/44128/2008) and financial support of the project MIT/ECE/0047/2009. This work used (Genomics or Cell Biology & Bioimaging) core facilities that are supported in part by COBRE (NIH-8 P20 GM103528) and NORC (NIH 1P30-DK072476) center grants from the National Institutes of Health. Authors would also like to acknowledge the following individuals: D'Andreas Williams for the histological processing of samples; Ana Rodrigues for kindly providing SEM images; João Requicha, Alessandra Zonari, Isabel Neto and specially Teresa Teigão for their help with the analysis of the histological images.

Abbreviation list

ASCs	Adipose-derived stromal/stem cells
BMP-2	Bone morphogenetic protein - 2
BMSCs	Bone marrow stromal/stem cells
BSA	Bovine serum albumin
CD	Cluster of differentiation
CT	Computed tomography
FBS	Fetal bovine serum
GMP	Good Manufacturing Practices
hASCs	Human adipose-derived stromal/stem cells
MSCs	Mesenchymal stromal/stem cells
PBS	Phosphate buffered saline
PCL	Poly-caprolactone
ROI	Region of interest
SD	Standard deviation
SPCL	Starch-polycaprolactone
SVF	Stromal vascular fraction

References

1. Fang TD, Nacamuli RP, Song HJ, Fong KD, Shi YY, Longaker MT. Guided tissue regeneration enhances bone formation in a rat model of failed osteogenesis. *Plast Reconstr Surg.* 2006; 117(4): 1177–85. [PubMed: 16582784]
2. Chim H, Schantz JT. New frontiers in calvarial reconstruction: integrating computer-assisted design and tissue engineering in cranioplasty. *Plast Reconstr Surg.* 2005; 116(6):1726–41. [PubMed: 16267439]
3. Gupta DM, Panetta NJ, Longaker MT. The use of polymer scaffolds in skeletal tissue engineering applications. *J Craniofac Surg.* 2009; 20(3):860–1. [PubMed: 19461326]
4. Guilak F, Lott KE, Awad HA, Cao Q, Hicok KC, Fermor B, Gimple JM. Clonal analysis of the differentiation potential of human adipose-derived adult stem cells. *J Cell Physiol.* 2006; 206(1): 229–37. [PubMed: 16021633]
5. Kwan MD, Slater BJ, Wan DC, Longaker MT. Cell-based therapies for skeletal regenerative medicine. *Hum Mol Genet.* 2008; 17(R1):R93–8. [PubMed: 18632703]
6. Xu Y, Malladi P, Wagner DR, Longaker MT. Adipose-derived mesenchymal cells as a potential cell source for skeletal regeneration. *Curr Opin Mol Ther.* 2005; 7(4):300–5. [PubMed: 16121695]
7. Panetta NJ, Gupta DM, Quarto N, Longaker MT. Mesenchymal cells for skeletal tissue engineering. *Panminerva Med.* 2009; 51(1):25–41. [PubMed: 19352307]
8. Huang JI, Zuk PA, Jones NF, Zhu M, Lorenz HP, Hedrick MH, Benhaim P. Chondrogenic potential of multipotential cells from human adipose tissue. *Plast Reconstr Surg.* 2004; 113(2):585–94. [PubMed: 14758221]
9. Zuk PA, Zhu M, Ashjian P, De Ugarte DA, Huang JI, Mizuno H, Alfonso ZC, Fraser JK, Benhaim P, Hedrick MH. Human adipose tissue is a source of multipotent stem cells. *Mol Biol Cell.* 2002; 13(12):4279–95. [PubMed: 12475952]

10. Gimble JM, Guilak F. Differentiation potential of adipose derived adult stem (ADAS) cells. *Curr Top Dev Biol.* 2003; 58:137–60. [PubMed: 14711015]
11. Gimble JM, Nuttall ME. Bone and fat: old questions, new insights. *Endocrine.* 2004; 23(2–3):183–8. [PubMed: 15146099]
12. Gimble JM, Zvonic S, Floyd ZE, Kassem M, Nuttall ME. Playing with bone and fat. *J Cell Biochem.* 2006; 98(2):251–66. [PubMed: 16479589]
13. Hicok KC, Du Laney TV, Zhou YS, Halvorsen YD, Hitt DC, Cooper LF, Gimble JM. Human adipose-derived adult stem cells produce osteoid in vivo. *Tissue Eng.* 2004; 10(3–4):371–80. [PubMed: 15165454]
14. Carvalho PP, Wu X, Yu G, Dias IR, Gomes ME, Reis RL, Gimble JM. The effect of storage time on adipose-derived stem cell recovery from human lipoaspirates. *Cells Tissues Organs.* 2011; 194(6):494–500. [PubMed: 21494019]
15. Dudas JR, Marra KG, Cooper GM, Penascino VM, Mooney MP, Jiang S, Rubin JP, Losee JE. The osteogenic potential of adipose-derived stem cells for the repair of rabbit calvarial defects. *Ann Plast Surg.* 2006; 56(5):543–8. [PubMed: 16641633]
16. Yoon E, Dhar S, Chun DE, Gharibjanian NA, Evans GR. In vivo osteogenic potential of human adipose-derived stem cells/poly lactide-co-glycolic acid constructs for bone regeneration in a rat critical-sized calvarial defect model. *Tissue Eng.* 2007; 13(3):619–27. [PubMed: 17518608]
17. Lendeckel S, Jodicke A, Christophis P, Heidinger K, Wolff J, Fraser JK, Hedrick MH, Berthold L, Howaldt HP. Autologous stem cells (adipose) and fibrin glue used to treat widespread traumatic calvarial defects: case report. *J Craniomaxillofac Surg.* 2004; 32(6):370–3. [PubMed: 1555520]
18. Scaglione M, Fabbri L, Dell’omo D, Gambini F, Guido G. Long bone nonunions treated with autologous concentrated bone marrow-derived cells combined with dried bone allograft. *Musculoskelet Surg.* 2013
19. Stromberg A, Jansson M, Fischer H, Rullman E, Hagglund H, Gustafsson T. Bone marrow derived cells in adult skeletal muscle tissue in humans. *Skelet Muscle.* 2013; 3(1):12. [PubMed: 23680018]
20. Backly RM, Cancedda R. Bone marrow stem cells in clinical application: harnessing paracrine roles and niche mechanisms. *Adv Biochem Eng Biotechnol.* 2010; 123:265–92. [PubMed: 20803145]
21. Levi B, James AW, Nelson ER, Hu S, Sun N, Peng M, Wu J, Longaker MT. Studies in adipose-derived stromal cells: migration and participation in repair of cranial injury after systemic injection. *Plast Reconstr Surg.* 2011; 127(3):1130–40. [PubMed: 21364416]
22. Levi B, James AW, Nelson ER, Vistnes D, Wu B, Lee M, Gupta A, Longaker MT. Human adipose derived stromal cells heal critical size mouse calvarial defects. *PLoS One.* 2010; 5(6):e11177. [PubMed: 20567510]
23. Cowan CM, Shi YY, Aalami OO, Chou YF, Mari C, Thomas R, Quarto N, Contag CH, Wu B, Longaker MT. Adipose-derived adult stromal cells heal critical-size mouse calvarial defects. *Nature Biotechnology.* 2004; 22(5):560–7.
24. Gamie Z, Tran GT, Vyzas G, Korres N, Heliotis M, Mantalaris A, Tsiridis E. Stem cells combined with bone graft substitutes in skeletal tissue engineering. *Expert Opin Biol Ther.*
25. Zippel N, Schulze M, Tobiasch E. Biomaterials and mesenchymal stem cells for regenerative medicine. *Recent Pat Biotechnol.* 4(1):1–22. [PubMed: 20201799]
26. Gosain AK, Santoro TD, Song LS, Capel CC, Sudhakar PV, Matloub HS. Osteogenesis in calvarial defects: contribution of the dura, the pericranium, and the surrounding bone in adult versus infant animals. *Plast Reconstr Surg.* 2003; 112(2):515–27. [PubMed: 12900610]
27. Levi B, James AW, Nelson ER, Li S, Peng M, Commons GW, Lee M, Wu B, Longaker MT. Human adipose-derived stromal cells stimulate autogenous skeletal repair via paracrine Hedgehog signaling with calvarial osteoblasts. *Stem Cells Dev.* 2011; 20(2):243–57. [PubMed: 20698749]
28. Levi B, James AW, Nelson ER, Peng M, Wan DC, Commons GW, Lee M, Wu B, Longaker MT. Acute skeletal injury is necessary for human adipose-derived stromal cell-mediated calvarial regeneration. *Plast Reconstr Surg.* 2011; 127(3):1118–29. [PubMed: 21364415]
29. Levi B, Nelson ER, Li S, James AW, Hyun JS, Montoro DT, Lee M, Glotzbach JP, Commons GW, Longaker MT. Dura mater stimulates human adipose-derived stromal cells to undergo bone formation in mouse calvarial defects. *Stem Cells.* 2011; 29(8):1241–55. [PubMed: 21656608]

30. Kim HP, Ji YH, Rhee SC, Dhong ES, Park SH, Yoon ES. Enhancement of bone regeneration using osteogenic-induced adipose-derived stem cells combined with demineralized bone matrix in a rat critically-sized calvarial defect model. *Curr Stem Cell Res Ther.* 2012; 7(3):165–72. [PubMed: 22329583]
31. Choi JW, Park EJ, Shin HS, Shin IS, Ra JC, Koh KS. In Vivo Differentiation of Undifferentiated Human Adipose Tissue-Derived Mesenchymal Stem Cells in Critical-Sized Calvarial Bone Defects. *Ann Plast Surg.* 2012
32. Bodde EW, Habraken WJ, Mikos AG, Spauwen PH, Jansen JA. Effect of polymer molecular weight on the bone biological activity of biodegradable polymer/calcium phosphate cement composites. *Tissue Eng Part A.* 2009; 15(10):3183–91. [PubMed: 19364281]
33. Rodrigues AI, Gomes ME, Leonor IB, Reis RL. Bioactive starch-based scaffolds and human adipose stem cells are a good combination for bone tissue engineering. *Acta Biomater.* 2012; 8(10):3765–76. [PubMed: 22659174]
34. Santos TC, Marques AP, Horing B, Martins AR, Tuzlakoglu K, Castro AG, van Griensven M, Reis RL. In vivo short-term and long-term host reaction to starch-based scaffolds. *Acta Biomater.* 2010; 6(11):4314–26. [PubMed: 20601228]
35. Gupta DM, Kwan MD, Slater BJ, Wan DC, Longaker MT. Applications of an athymic nude mouse model of nonhealing critical-sized calvarial defects. *J Craniofac Surg.* 2008; 19(1):192–7. [PubMed: 18216688]
36. Dubois SG, Floyd EZ, Zvonic S, Kilroy G, Wu X, Carling S, Halvorsen YD, Ravussin E, Gimble JM. Isolation of human adipose-derived stem cells from biopsies and liposuction specimens. *Methods Mol Biol.* 2008; 449:69–79. [PubMed: 18370084]
37. Carvalho PP, Wu X, Yu G, Dietrich M, Dias IR, Gomes ME, Reis RL, Gimble JM. Use of animal protein-free products for passaging adherent human adipose-derived stromal/stem cells. *Cytotherapy.* 2011; 13(5):594–7. [PubMed: 21198335]
38. Gronthos S, Franklin DM, Leddy HA, Robey PG, Storms RW, Gimble JM. Surface protein characterization of human adipose tissue-derived stromal cells. *J Cell Physiol.* 2001; 189(1):54–63. [PubMed: 11573204]
39. Aust L, Devlin B, Foster SJ, Halvorsen YD, Hicok K, du Laney T, Sen A, Willingmyre GD, Gimble JM. Yield of human adipose-derived adult stem cells from liposuction aspirates. *Cytotherapy.* 2004; 6(1):7–14. [PubMed: 14985162]
40. Dominici M, Le Blanc K, Mueller I, Slaper-Cortenbach I, Marini F, Krause D, Deans R, Keating A, Prockop D, Horwitz E. Minimal criteria for defining multipotent mesenchymal stromal cells. The International Society for Cellular Therapy position statement. *Cytotherapy.* 2006; 8(4):315–7. [PubMed: 16923606]
41. Halvorsen YD, Bond A, Sen A, Franklin DM, Lea-Currie YR, Sujkowski D, Ellis PN, Wilkison WO, Gimble JM. Thiazolidinediones and glucocorticoids synergistically induce differentiation of human adipose tissue stromal cells: biochemical, cellular, and molecular analysis. *Metabolism.* 2001; 50(4):407–13. [PubMed: 11288034]
42. Halvorsen YD, Franklin D, Bond AL, Hitt DC, Aughter C, Boskey AL, Paschalis EP, Wilkison WO, Gimble JM. Extracellular matrix mineralization and osteoblast gene expression by human adipose tissue-derived stromal cells. *Tissue Eng.* 2001; 7(6):729–41. [PubMed: 11749730]
43. Leonor IB, Rodrigues MT, Gomes ME, Reis RL. In situ functionalization of wet-spun fibre meshes for bone tissue engineering. *J Tissue Eng Regen Med.* 2011; 5(2):104–11. [PubMed: 20653041]
44. Tuzlakoglu K, Pashkuleva I, Rodrigues MT, Gomes ME, van Lenthe GH, Muller R, Reis RL. A new route to produce starch-based fiber mesh scaffolds by wet spinning and subsequent surface modification as a way to improve cell attachment and proliferation. *J Biomed Mater Res A.* 2010; 92(1):369–77. [PubMed: 19191314]
45. Yu G, Wu X, Dietrich MA, Polk P, Scott LK, Ptitsyn AA, Gimble JM. Yield and characterization of subcutaneous human adipose-derived stem cells by flow cytometric and adipogenic mRNA analyzes. *Cytotherapy.* 2010; 12(4):538–46. [PubMed: 20380539]
46. Zuk PA, Zhu M, Mizuno H, Huang J, Futrell JW, Katz AJ, Benhaim P, Lorenz HP, Hedrick MH. Multilineage cells from human adipose tissue: implications for cell-based therapies. *Tissue Eng.* 2001; 7(2):211–28. [PubMed: 11304456]

47. Amini AR, Laurencin CT, Nukavarapu SP. Bone tissue engineering: recent advances and challenges. *Crit Rev Biomed Eng.* 2012; 40(5):363–408. [PubMed: 23339648]
48. Bose S, Roy M, Bandyopadhyay A. Recent advances in bone tissue engineering scaffolds. *Trends Biotechnol.* 2012; 30(10):546–54. [PubMed: 22939815]
49. Santos MI, Fuchs S, Gomes ME, Unger RE, Reis RL, Kirkpatrick CJ. Response of micro- and macrovascular endothelial cells to starch-based fiber meshes for bone tissue engineering. *Biomaterials.* 2007; 28(2):240–8. [PubMed: 16945411]
50. Rodrigues MT, Gomes ME, Viegas CA, Azevedo JT, Dias IR, Guzon FM, Reis RL. Tissue-engineered constructs based on SPCL scaffolds cultured with goat marrow cells: functionality in femoral defects. *J Tissue Eng Regen Med.* 2011; 5(1):41–9. [PubMed: 20603869]
51. Rada T, Santos TC, Marques AP, Correlo VM, Frias AM, Castro AG, Neves NM, Gomes ME, Reis RL. Osteogenic differentiation of two distinct subpopulations of human adipose-derived stem cells: an in vitro and in vivo study. *J Tissue Eng Regen Med.* 2012; 6(1):1–11. [PubMed: 21294275]
52. Araujo JV, Cunha-Reis C, Rada T, da Silva MA, Gomes ME, Yang Y, Ashammakhi N, Reis RL, El-Haj AJ, Neves NM. Dynamic culture of osteogenic cells in biomimetically coated poly(caprolactone) nanofibre mesh constructs. *Tissue Eng Part A.* 2010; 16(2):557–63. [PubMed: 19728792]
53. Rodrigues MT, Lee SJ, Gomes ME, Reis RL, Atala A, Yoo JJ. Bilayered constructs aimed at osteochondral strategies: the influence of medium supplements in the osteogenic and chondrogenic differentiation of amniotic fluid-derived stem cells. *Acta Biomater.* 2012; 8(7):2795–806. [PubMed: 22510402]
54. Link DP, Gardel LS, Correlo VM, Gomes ME, Reis RL. Osteogenic properties of starch poly(epsilon-caprolactone) (SPCL) fiber meshes loaded with osteoblast-like cells in a rat critical-sized cranial defect. *J Biomed Mater Res A.* 2013
55. Cornejo A, Sahar DE, Stephenson SM, Chang S, Nguyen S, Guda T, Wenke JC, Vasquez A, Michalek JE, Sharma R, et al. Effect of adipose tissue-derived osteogenic and endothelial cells on bone allograft osteogenesis and vascularization in critical-sized calvarial defects. *Tissue Eng Part A.* 2012; 18(15–16):1552–61. [PubMed: 22440012]
56. Lin Y, Tang W, Wu L, Jing W, Li X, Wu Y, Liu L, Long J, Tian W. Bone regeneration by BMP-2 enhanced adipose stem cells loading on alginate gel. *Histochem Cell Biol.* 2008; 129(2):203–10. [PubMed: 17978832]
57. Bohnenblust ME, Steigelman MB, Wang Q, Walker JA, Wang HT. An experimental design to study adipocyte stem cells for reconstruction of calvarial defects. *J Craniofac Surg.* 2009; 20(2): 340–6. [PubMed: 19242366]

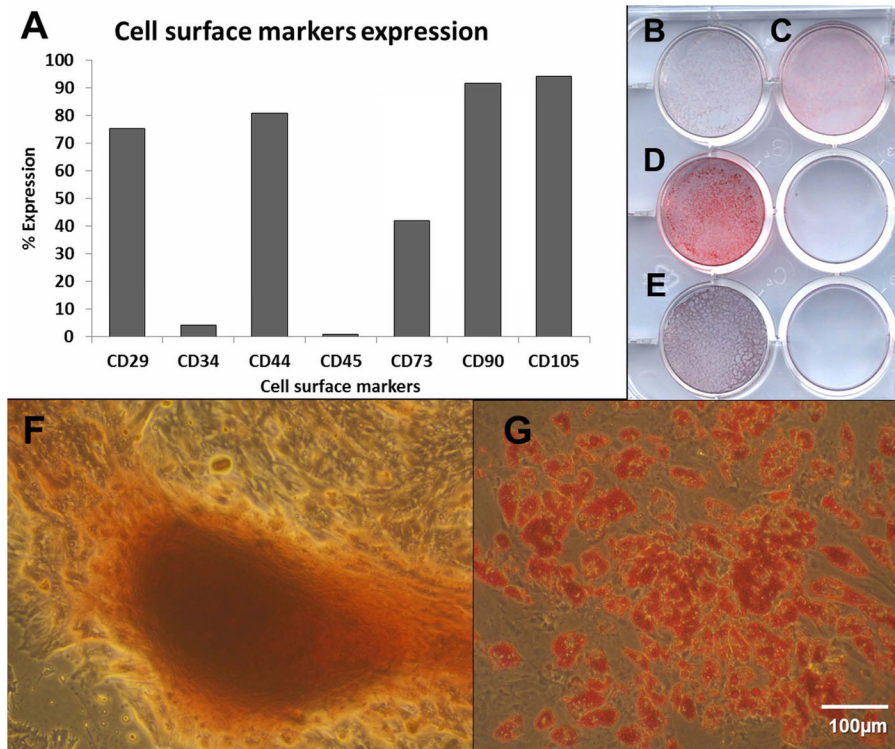


Fig. 1. **A)** Flow Cytometry analysis of cell surface markers of the pool of ASCs. **B–E)** - Macrophotographs of ASCs differentiation in cultured in well-plate: **B)** osteogenic control; **C)** adipogenic control; **D)** adipogenic differentiation (Oil Red O staining) and; **E)** osteogenic differentiation (Alizarin Red staining). **F-G)** – Microphotographs of osteogenic (F – Alizarin Red staining) and adipogenic (G – Oil Red O staining) differentiation ability of pool of ASCs (from 5 donors).

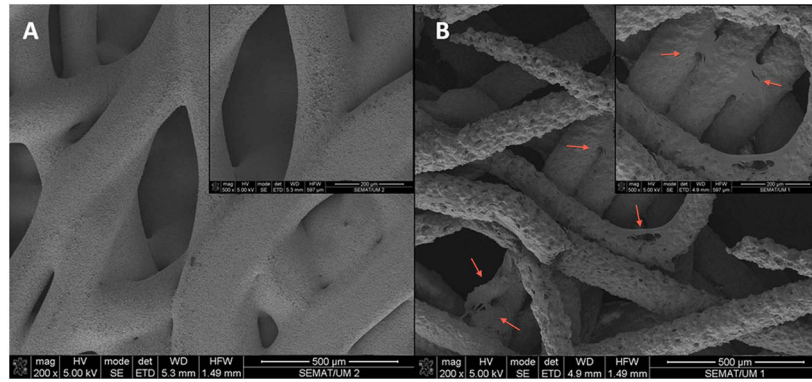


Fig. 2. SEM microphotographs of SPCL scaffolds

A – SPCL scaffold alone; **B** – SPCL scaffold loaded with ASCs (magnifications of each image on upper right corners). Red arrows pointing some of the ASCs spread on SPCL fibers.

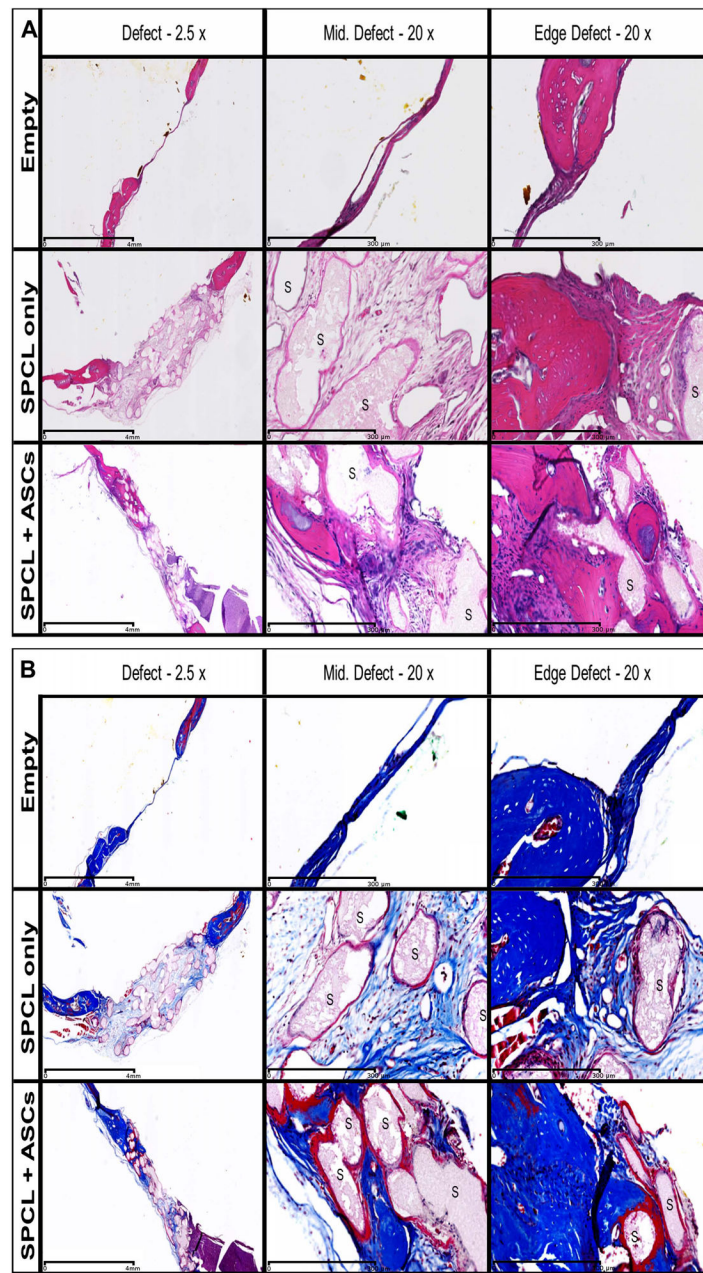


Fig. 3. Histology of the explants

Serial sections of the defect site explants at 8 weeks after implantation of the constructs. Sections were stained with **A** - Hematoxylin/Eosin (osteoid and nuclei were stained dark pink and dark purple respectively) and **B** - Masson's Trichrome (osteoid stained blue, nuclei stained black and cytoplasm stained red). Representative images for empty defects, SPCL scaffold alone and SPCL scaffold with ASCs are shown. "S" represents SPCL fibers. First column shows the general defect site with 2.5x magnification (scale bar represents 4 mm). Second and third columns represent the middle and one of the edges of the defect, respectively. 20x magnification (scale bar represents 300 μ m).

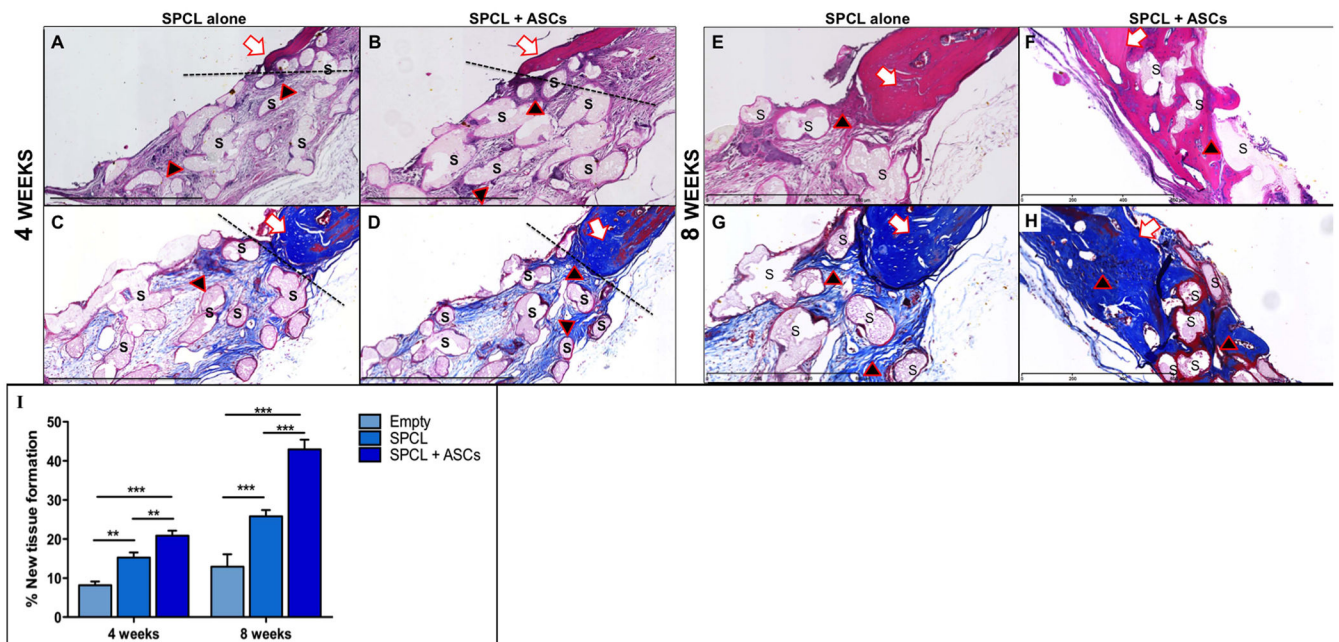


Fig. 4. Detail of histological images of the explants

White arrows indicate original bone; black arrows indicate new tissue formation; “S” indicates SPCL fibers. **A, B, E** and **F** are H&E staining (**A** and **B** at 4 weeks; **E** and **F** at 8 weeks); **C, D, G** and **H** are Masson’s Trichrome staining (**C** and **D** at 4 weeks; **G** and **H** at 8 weeks); **discontinued line (- - -)** outlines the interface of the native bone and the defect. **I - Histomorphometric analysis.** Two-way ANOVA was performed on measurements of 4 histological sections for each group at each time-point. ** represents $p < 0.01$; *** represents $p < 0.001$.

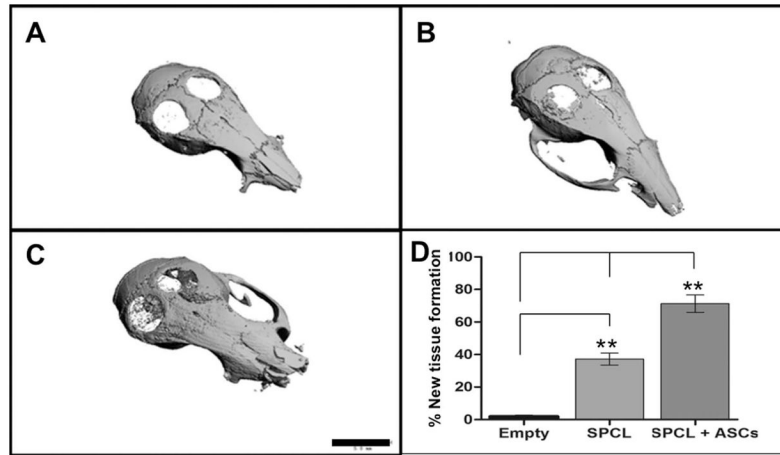


Fig. 5. Micro-CT images

Representative 3D reconstructed images after 8 weeks of: **A**- Empty defects; **B** – SPCL scaffolds alone; **C** – SPCL scaffolds with ASCs. Black bar represents 5.0 mm. **D** – Chart representing percentage of mineralized tissue present on total area of the defects (ROI was determined covering the entire defect area) (n = 3 defects per group). Values presented as mean ± SD. Significance measured by one-way ANOVA where ** represents p < 0.01.